

SDM-PEB: Spatial-Depthwise Mamba for Enhanced Post-Exposure Bake Simulation

Ziyang Yu¹, Peng Xu¹, Zixiao Wang¹, Binwu Zhu², Qipan Wang³, Yibo Lin³, Runsheng Wang³, Bei Yu¹, Martin Wong⁴

¹The Chinese University of Hong Kong ²Southeast University&NCTIEDA
³Peking University ⁴Hong Kong Baptist University

Highlights

- Precise & Fast PEB Modeling: We introduce SDM-PEB, a streamlined pipeline for accurate, high-speed post-exposure-bake simulation.
- Hierarchical ViT Encoder: Extracts multi-scale spatial features within each photoacid depth layer.
- Spatial-Depthwise Mamba Attention: A lightweight unit that captures cross-depth dependencies efficiently.
- PEB Focal Loss & Depthwise Divergence Reg.: Tailored objectives that handle data imbalance and refine layer-wise learning.
- Industry Validation: On S-Litho benchmarks, SDM-PEB outperforms existing methods in both accuracy and runtime.

Background and Motivation

Predictive Lithography Simulation comprises two key stages:

- Optical Simulation: models light-mask interaction and pattern projection onto the photoresist.
- Photoresist Simulation: captures resist chemistry and physics from exposure, through post-exposure bake (PEB), to final development.

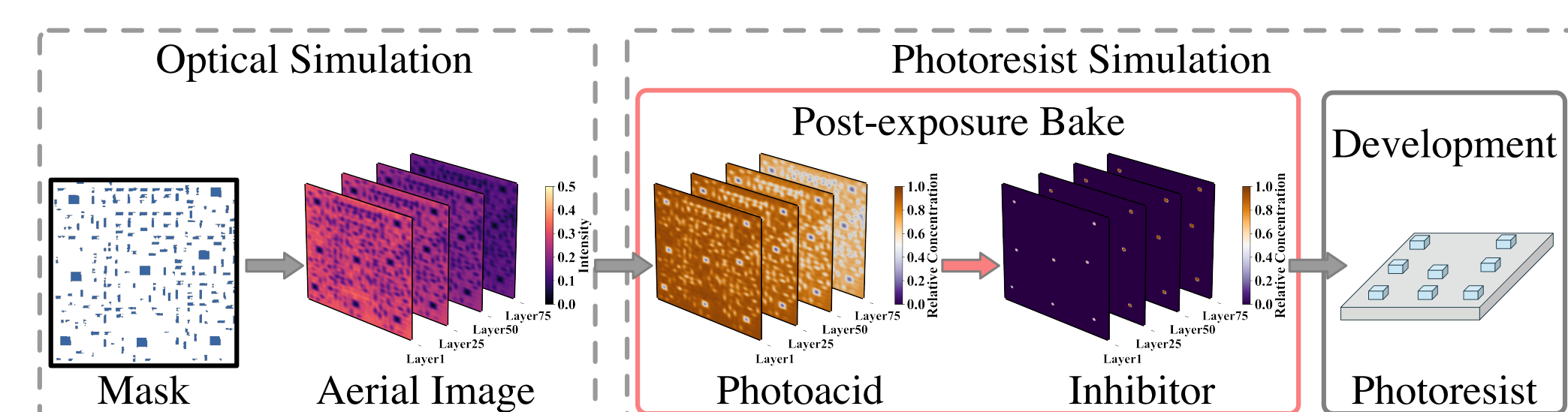


Figure 1. A typical flow of lithography simulation for chemically amplified resist: from optical simulation to photoresist simulation.

Post-Exposure Bake Process: Thermal-driven PEB process for chemically amplified resist contain

- Catalytic reaction between inhibitor [\mathcal{I}] and photoacid [\mathcal{A}] Equation (1),
- neutralization-diffusion between photoacid and base quencher [\mathcal{B}] Equation (2),
- photoresist development with rate R Equation (4).

$$\frac{\partial[\mathcal{I}]}{\partial t} = -k_c[\mathcal{I}][\mathcal{A}], \quad (1)$$

$$\frac{\partial[\mathcal{A}]}{\partial t} = -k_r[\mathcal{A}][\mathcal{B}] + D_{\mathcal{A}}\nabla^2[\mathcal{A}], \quad (2)$$

$$\frac{\partial[\mathcal{B}]}{\partial t} = -k_r[\mathcal{A}][\mathcal{B}] + D_{\mathcal{B}}\nabla^2[\mathcal{B}]. \quad (3)$$

$$\vec{R}(x, y, z) = R_{max} \frac{(a+1)(1-[\mathcal{I}])^n}{a+(1-[n])^n} + R_{min}, \quad a = (1-M_{th}) \frac{n+1}{n-1}. \quad (4)$$

Existing Problems:

- Finite element analysis (FEA) and finite difference methods (FDM) demand significant computational resources due to 3D distribution characteristic.
- DeePEB [2] cannot fully capture continuous spatial and depthwise dependencies in 3D space using FNO and CNN.

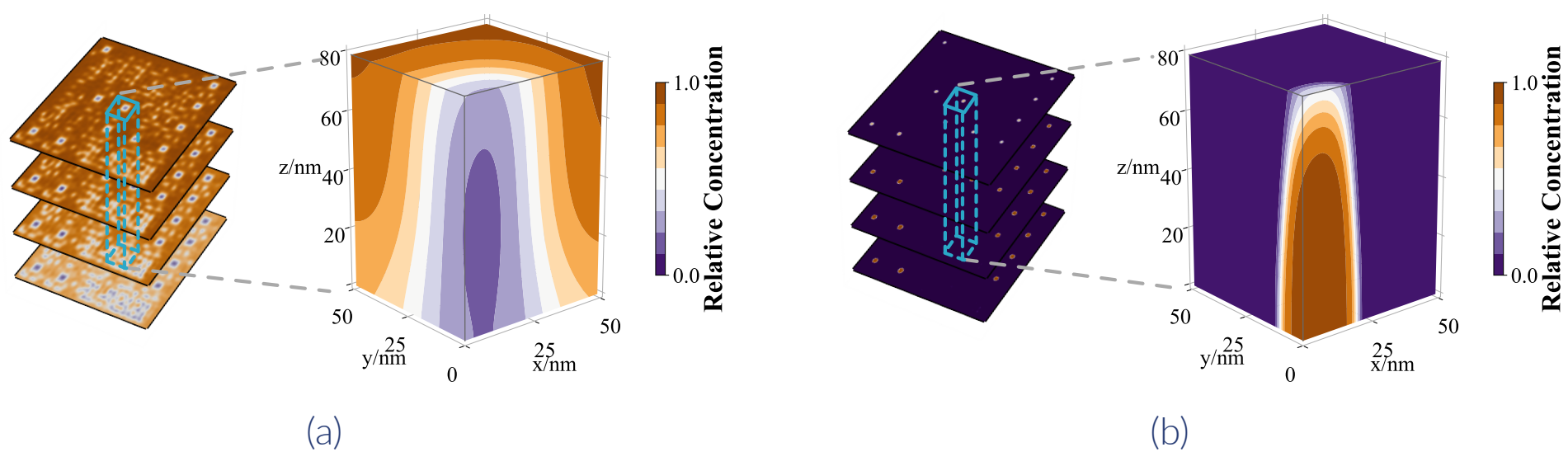


Figure 2. Vertical visualization of distributions: (a) photoacid at the initial stage and (b) inhibitor at the final stage.

State Space Models-based Methodologies

- Feature representations in 3D photoresist can be naturally modeled as sequences of depth-levels (from shallow to deep).
- Linear time-invariant SSM:** maps scalar input sequence x_t to scalar output y_t through hidden state $h_t \in \mathbb{R}^N$, for $t = 1, \dots, L$.
- Dynamics:** $h_{t+1} = A h_t + B x_t, \quad y_t = C^\top h_t$.
- Parameters:**
 - $A \in \mathbb{R}^{N \times N}$ – state matrix, HiPPO-initialized.
 - $B, C \in \mathbb{R}^{N \times 1}$ – input/output projection vectors.
- Mamba** ties SSM parameters to the input, spotlighting relevant signals and filtering out the rest.

$$\vec{B} = \text{Linear}_N(\vec{x}), \quad \vec{C} = \text{Linear}_N(\vec{x}), \quad (5)$$

$$\vec{\Delta} = \text{softplus}(\text{Broadcast}_K(\text{Linear}_1(\vec{x})) + \vec{D}), \quad (6)$$

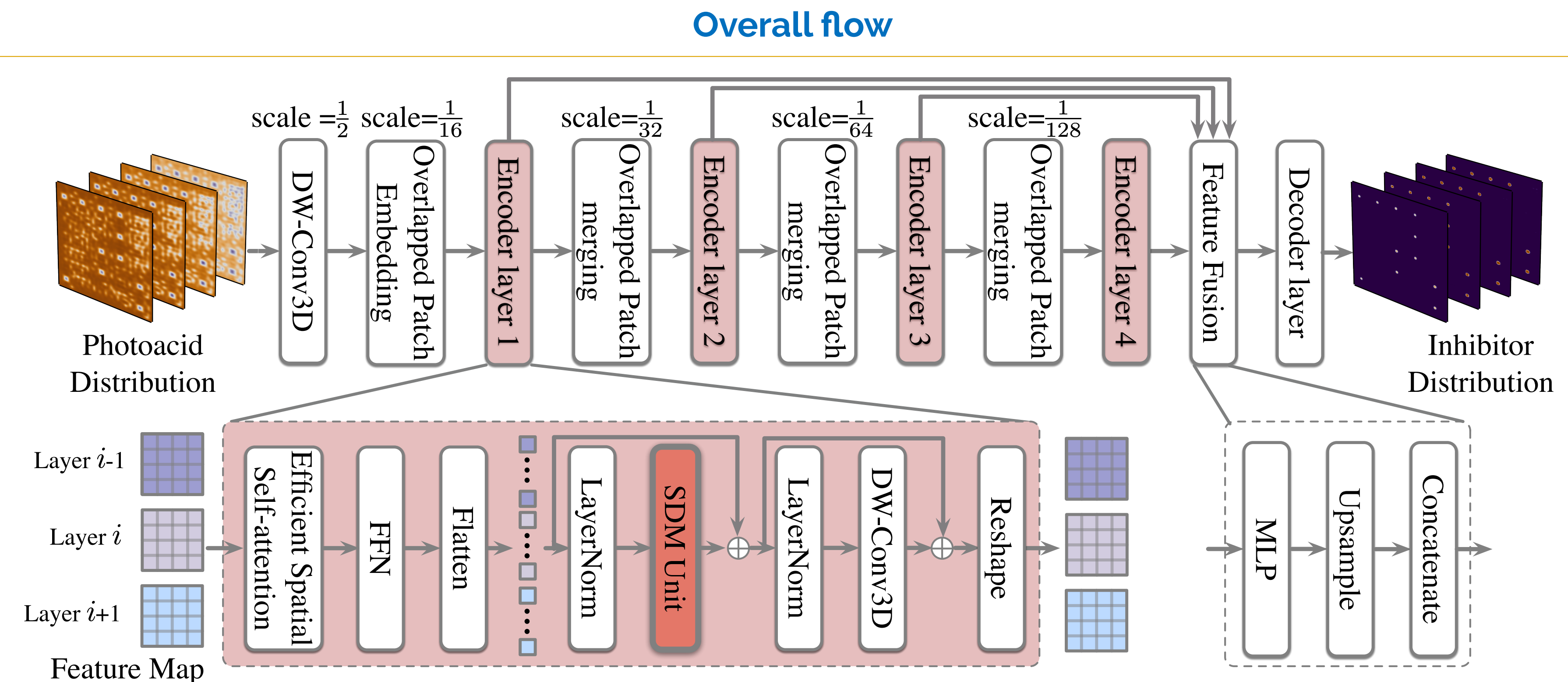


Figure 3. The architecture overview of our proposed SDM-PEB framework.

Hierarchical Contextual Feature Extractor

Depthwise Overlapped Patch Merging:

- Reduce information loss at patch boundaries

Efficient Spatial Self-Attention:

- C : feature dimension of \vec{K} ; r : reduction ratio
- Computational complexity: $O(L^2) \rightarrow O(L^2/r)$

$$\hat{\vec{K}} = \text{Reshape} \left(\frac{L}{r}, C \cdot r \right) (\vec{K}), \quad \vec{K} = \text{Linear}_C(\hat{\vec{K}}), \quad (7)$$

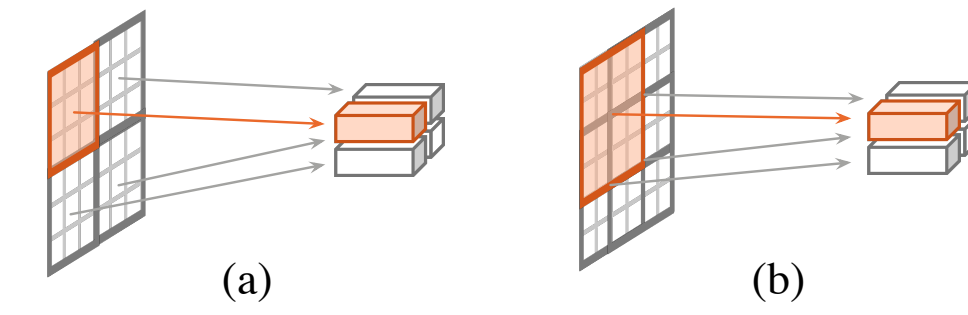


Figure 4. (a) Non-overlapped patch merging and (b) overlapped patch merging.

Spatial-Depthwise Mamba-based Attention Unit

Structure of SDM Unit:

- Input reshaping:** The i -th layer feature map is flattened to a sequence q_i and normalized.
- Dual projection:** q_i is linearly split into two streams x_i and z_i .
- Directional scans:** For every scan direction, x_i passes through a 1-D conv + SiLU to yield x'_i , which drives a spatial-depthwise selective scan.
- Attention fusion:** Scan outputs are gated by z_i and aggregated to form feature p_i , capturing inter-/intra-layer dependencies.

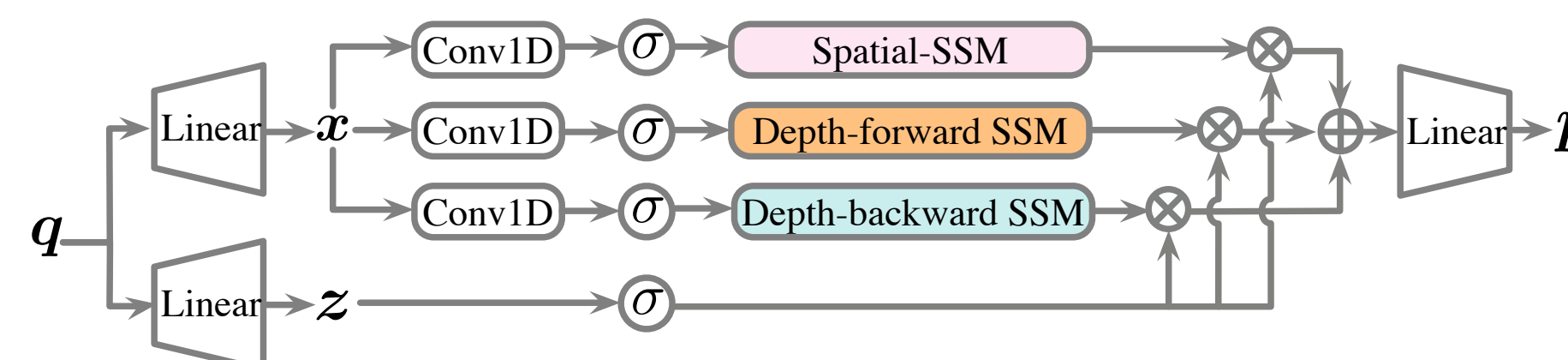


Figure 5. The architecture of the spatial-depthwise Mamba-based attention unit.

Spatial-Depthwise PEB Selective Scan:

- Spatial scan:** at a fixed (x, y) location, sweeps through all depth layers.
- Depth-Forward Scan:** traverses layers shallow \rightarrow deep
- Depth-Backward Scan:** traverses layers deep \rightarrow shallow (reverse of depth-forward)

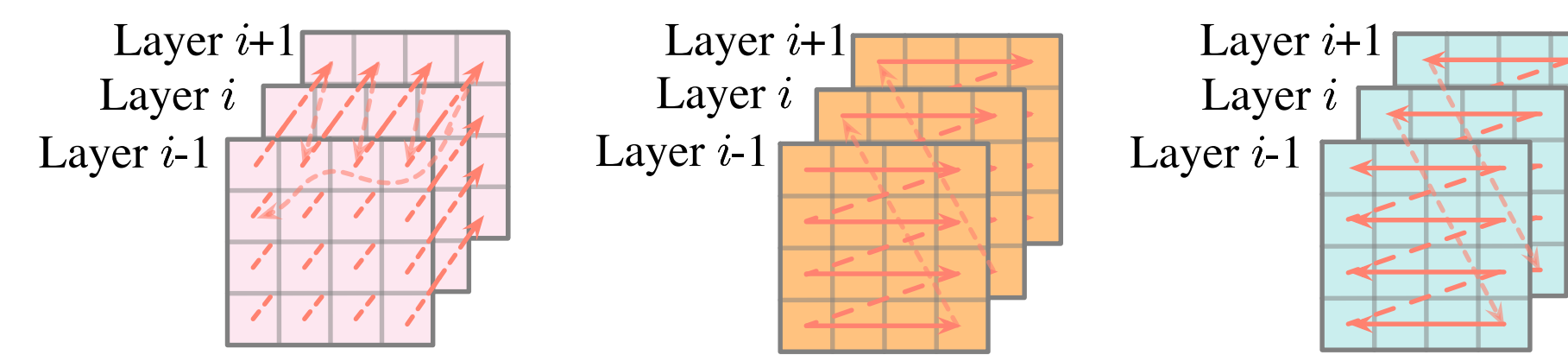


Figure 6. From left to right: spatial scan, depth-forward scan, and depthbackward scan.

Customized PEB Optimization Objectives

- Maximum squared error:** $\mathcal{L}_{\text{MaxSE}} = \max_{d,h,w} (\hat{y}_{d,h,w} - y_{d,h,w})^2$.

PEB focal loss:

$$\mathcal{L}_{\text{PEB-FL}} = \sum_d^D \sum_h^H \sum_w^W |\hat{y}_{d,h,w} - y_{d,h,w}|^\gamma (\hat{y}_{d,h,w} - y_{d,h,w})^2$$

Differential Depth Divergence Regularization:

$$\mathcal{L}_{\text{Div}} = \sum_{d=1}^{D-1} \sigma(\Delta \hat{y}_d) \log \frac{\sigma(\Delta \hat{y}_d)}{\sigma(\Delta y_d)}, \text{ where:}$$

$$\Delta y_d = y_{d+1} - y_d, \quad \sigma(\Delta y_d) = \frac{\exp(\Delta y_d/\tau)}{\sum_{h=1}^H \sum_{w=1}^W \exp(\Delta y_{d,h,w}/\tau)}$$

Evaluation Results

Table 1. Comparison with different PEB solvers.

Methodologies	Inhibitor RMSE (nm)	Inhibitor NRMSE (%)	Develop Rate RMSE (nm/s)	CD Error x (nm)	CD Error y (nm)	RT/s
DeepCNN [3]	8.25	12.53	0.65	1.63	3.14	6.26
TEMPO-resist [4]	7.67	12.55	0.50	1.26	2.12	2.45
FNO [1]	7.91	11.68	0.68	1.69	2.34	3.71
DeePEB [2]	3.99	5.70	0.48	1.19	0.98	1.24
SDM-PEB	2.78	3.70	0.35	0.86	0.74	0.93

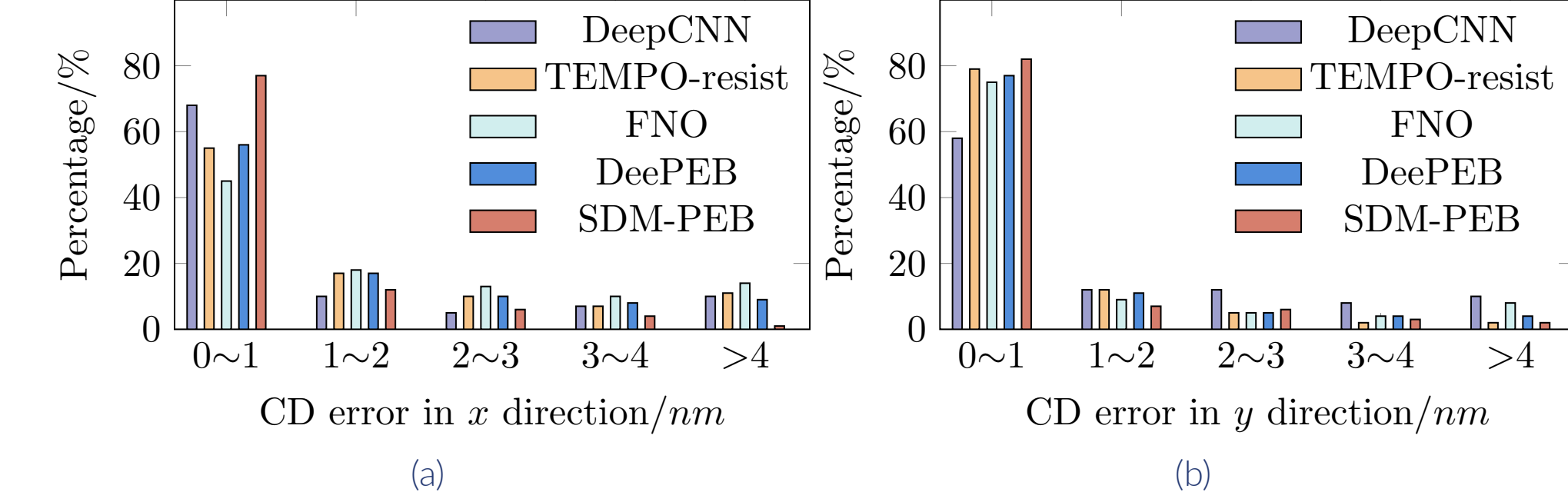


Figure 7. Percentage counts of CD errors using different methods: (a) error in the x direction and (b) error in the y direction.

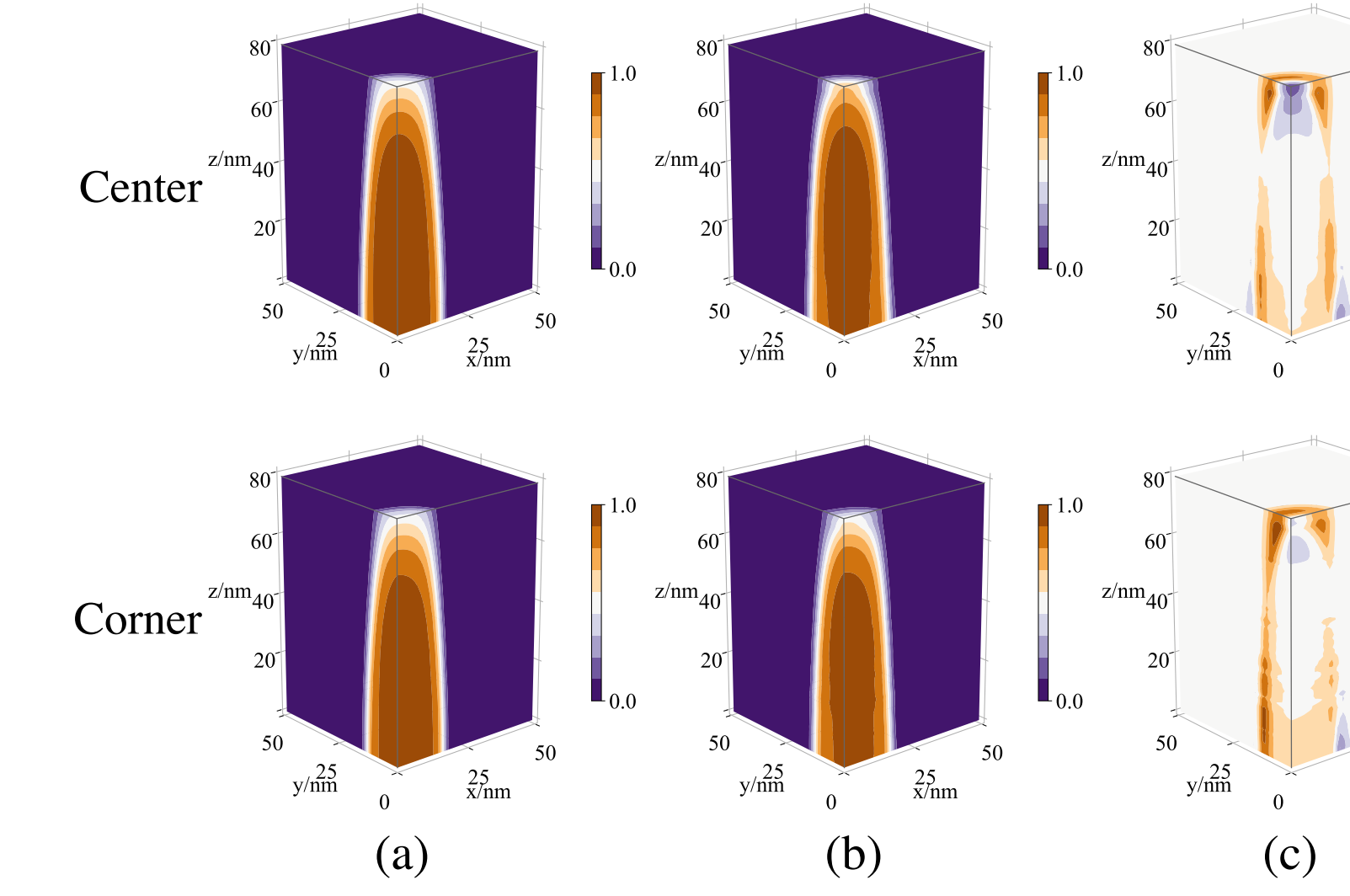


Figure 8. Vertical visualization of predicted results: the upper row shows the center contact, the lower row shows the corner contact. (a) Ground truths, (b) predictions, (c) differences.

References

- Zongyi Li, Nikola Kovachki, Kamran Azizzadenesheli, Burigede Liu, Kaushik Bhattacharya, Andrew Stuart, and Anima Anandkumar. Fourier neural operator for parametric partial differential equations. *arXiv preprint arXiv:2010.08895*, 2020.
- Qipan Wang, Xiaohan Gao, Yibo Lin, Runsheng Wang, and Ru Huang. Deepeb: A neural partial differential equation solver for post exposure baking simulation in lithography. In *Proceedings of the 41st IEEE/ACM International Conference on Computer-Aided Design*, pages 1–9, 2022.
- Yuki Watanabe, Taiki Kimura, Tetsuaki Matsunawa, and Shigeki Nojima. Accurate lithography simulation model based on convolutional neural networks. In *Optical Microlithography XXX*, volume 10147, pages 137–145. SPIE, 2017.
- Wei Ye, Mohamed Baker Alawieh, Yuki Watanabe, Shigeki Nojima, Yibo Lin, and David Z Pan. Tempo: Fast mask topography effect modeling with deep learning. In *Proceedings of the 2020 International Symposium on Physical Design*, pages 127–134, 2020.